



ARTICLE

Expanded phenotype of *AARS1*-related white matter disease

Guy Helman^{1,2}, Marisa I. Mendes³, Francesco Nicita⁴, Lama Darbelli^{5,6,7,8}, Omar Sherbini⁹, Travis Moore^{5,6}, Alexa Derksen^{5,6}, Amy Pizzino⁹, Rosalba Carrozzo⁴, Alessandra Torracio⁴, Michela Catteruccia⁴, Chiara Aiello⁴, Paola Goffrini¹⁰, Sonia Figuccia¹⁰, Desiree E. C. Smith³, Kinga Hadzsiev¹¹, Andreas Hahn¹², Saskia Biskup¹³, Ines Brösse¹⁴, Urania Kotzaeridou¹⁴, Darja Gauck¹⁵, Theresa A. Grebe¹⁶, Frances Elmslie¹⁷, Karen Stals¹⁸, Rajat Gupta¹⁹, Enrico Bertini⁴, Isabelle Thiffault^{20,21,22}, Ryan J. Taft²³, Raphael Schiffmann²⁴, Ulrich Brandl²⁵, Tobias B. Haack¹⁵, Gajja S. Salomons³, Cas Simons^{1,2}, Geneviève Bernard^{5,6,7,8}, Marjo S. van der Knaap^{26,27}, Adeline Vanderver^{9,28,29}✉ and Ralf A. Husain^{25,29}✉

PURPOSE: Recent reports of individuals with cytoplasmic transfer RNA (tRNA) synthetase-related disorders have identified cases with phenotypic variability from the index presentations. We sought to assess phenotypic variability in individuals with *AARS1*-related disease.

METHODS: A cross-sectional survey was performed on individuals with biallelic variants in *AARS1*. Clinical data, neuroimaging, and genetic testing results were reviewed. Alanine tRNA synthetase (AlaRS) activity was measured in available fibroblasts.

RESULTS: We identified 11 affected individuals. Two phenotypic presentations emerged, one with early infantile-onset disease resembling the index cases of *AARS1*-related epileptic encephalopathy with deficient myelination ($n = 7$). The second ($n = 4$) was a later-onset disorder, where disease onset occurred after the first year of life and was characterized on neuroimaging by a progressive posterior predominant leukoencephalopathy evolving to include the frontal white matter. AlaRS activity was significantly reduced in five affected individuals with both early infantile-onset and late-onset phenotypes.

CONCLUSION: We suggest that variants in *AARS1* result in a broader clinical spectrum than previously appreciated. The predominant form results in early infantile-onset disease with epileptic encephalopathy and deficient myelination. However, a subgroup of affected individuals manifests with late-onset disease and similarly rapid progressive clinical decline. Longitudinal imaging and clinical follow-up will be valuable in understanding factors affecting disease progression and outcome.

Genetics in Medicine (2021) 23:2352–2359; <https://doi.org/10.1038/s41436-021-01286-8>

INTRODUCTION

Variants in genes encoding cytoplasmic and mitochondrial aminoacyl-transfer RNA synthetases (aaRSs) have been implicated in a series of heritable neurologic conditions. AaRSs make up a group of ubiquitously expressed, essential enzymes that play a role in the first step of protein translation through the charging of tRNA molecules with their cognate amino acids. In general, each amino acid is coupled to its own charging enzyme and these enzymes are primarily encoded by two gene groups with function either primarily in the cytoplasm (designated -*ARS1*, whereby it should be noted that “-” in -*ARS1* stands for the corresponding amino acid in the one-letter code, e.g., a cytoplasmic aminoacyl-tRNA synthetase for alanine is encoded by *AARS1*, for arginine by

RARS1) or in mitochondria (designated -*ARS2*) [1, 2]. Recently, these genes have been associated with dominant and/or recessive forms of diseases that are thought to arise due to dysfunction in tRNA charging activity and the inability to meet high translational demand [1, 3].

A recent deep phenotyping study of recessive -*ARS1* defects demonstrated that all identified disorders were associated with central nervous system (CNS) signs or impairment of sensory functions such as hearing and/or vision. In most cases, individuals presented with failure to thrive, feeding, and gastrointestinal problems [3]. Liver disease, facial dysmorphism, various endocrine abnormalities, and mitochondrial dysfunction were reported for >30% of the different -*ARS1* defects [3]. Often, this pattern of

¹Murdoch Children's Research Institute, The Royal Children's Hospital, Parkville, VIC, Australia. ²Institute for Molecular Bioscience, The University of Queensland, Brisbane, Queensland, Australia. ³Metabolic Unit, Department of Clinical Chemistry, Amsterdam UMC, Vrije Universiteit Amsterdam, Amsterdam, The Netherlands. ⁴Department of Neurosciences, Unit of Muscular and Neurodegenerative Disorders, Laboratory of Molecular Medicine, Bambino Gesù Children's Hospital, IRCCS, Rome, Italy. ⁵Department of Neurology and Neurosurgery, McGill University, Montreal, QC, Canada. ⁶Child Health and Human Development Program, Research Institute of the McGill University Health Centre, Montreal, QC, Canada. ⁷Department of Pediatrics, McGill University, Montreal, QC, Canada. ⁸Department of Human Genetics, McGill University, Montreal, QC, Canada. ⁹Division of Neurology, Children's Hospital of Philadelphia, Philadelphia, PA, USA. ¹⁰Department of Chemistry, Life Sciences and Environmental Sustainability, University of Parma, Parma, Italy. ¹¹Department of Medical Genetics, University of Pécs, Pécs, Hungary. ¹²Department of Child Neurology, Justus-Liebig-University, Giessen, Germany. ¹³Praxis fuer Humangenetik und CeGaT GmbH, Tuebingen, Germany. ¹⁴Division of Child Neurology and Inherited Metabolic Diseases, Centre for Paediatrics and Adolescent Medicine, University Hospital Heidelberg, Heidelberg, Germany. ¹⁵Institute of Medical Genetics and Applied Genomics, University of Tuebingen, Tuebingen, Germany. ¹⁶Division of Genetics and Metabolism, Department of Child Health, Phoenix Children's Hospital, University of Arizona College of Medicine, Phoenix, AZ, USA. ¹⁷South West Thames Regional Genetics Service, St George's University Hospital, London, UK. ¹⁸Molecular Genetics Department, Royal Devon and Exeter NHS Foundation Trust, Exeter, UK. ¹⁹Department of Neurology, Birmingham Children's Hospital, Birmingham, UK. ²⁰Children's Mercy Kansas City, Center for Pediatric Genomic Medicine, Kansas City, MO, USA. ²¹Department of Pathology and Laboratory Medicine, Children's Mercy Hospitals, Kansas City, MO, USA. ²²School of Medicine, University of Missouri-Kansas City, Kansas City, MO, USA. ²³illumina, Inc, San Diego, CA, USA. ²⁴Baylor Scott & White Research Institute, Dallas, TX, USA. ²⁵Department of Neuropediatrics, Jena University Hospital, Jena, Germany. ²⁶Department of Child Neurology, Emma Children's Hospital, Amsterdam University Medical Centers, Vrije Universiteit Amsterdam and Amsterdam Neuroscience, Amsterdam, The Netherlands. ²⁷Department of Functional Genomics, Center for Neurogenomics and Cognitive Research, VU University, Amsterdam, The Netherlands. ²⁸Department of Neurology, University of Pennsylvania, Perelman School of Medicine, Philadelphia, PA, USA. ²⁹Shared Senior Authors: Adeline Vanderver and Ralf A. Husain. ✉email: vandervera@email.chop.edu; Ralf.Husain@med.uni-jena.de

severe multisystem disease occurred in the first months of life and was concurrent with periods of stress, particularly infection [3].

For many of the recessive *AARS1*-related disorders, the earliest reports revealed unique phenotypes that permitted the grouping of patients and identification of disease [4–6]. However, increased identification of affected individuals with variants in these genes has revealed significant phenotypic diversity among individuals with variants in *AARS1* genes. As genomic evaluation continues to grow in the diagnostic workup of patients, knowledge of the phenotypic spectrum of a given disorder can help to corroborate genetic findings [7], in particular in the absence of absolute evidence regarding the pathogenicity of an identified variant.

AARS1 encodes the cytoplasmic aminoacyl-tRNA synthetase for alanine (AlaRS) and has been previously associated with dominant and recessive disease. Heterozygous variants in *AARS1* are associated with a dominant form of Charcot–Marie–Tooth disease, type 2N (CMT2N [OMIM 613287]). In the case of recessive *AARS1*-related disease (OMIM 616339), the index cases had a distinct clinical presentation, with early infantile epileptic encephalopathy, deficient cerebral myelination, and peripheral neuropathy [5]. Subsequent reports of four individuals from three families with *AARS1*-related disease matched this phenotype [8–10] and a more recent report revealed recurrent acute liver failure in a single case [11]. Here we present data on 11 additional individuals from 10 families with biallelic variants in *AARS1*. We provide insight into a divergent presentation of recessive *AARS1*-related disease through clinical and neuroimaging evidence in cases with atypical presentations. Further, we provide functional assessment of AlaRS aminoacylation activity in five individuals.

MATERIALS AND METHODS

Patient recruitment

Patients and their families were collected prospectively in the Myelin Disorders Bioregistry Project (MDBP). Written informed consent for collection of clinical information, neuroimaging, and genetic information was obtained for each study participant.

Abstraction of clinical data

Clinical and demographic data were abstracted from available medical records of affected individuals. Neuroimaging was reviewed for all cases where available. Genetic testing reports were reviewed or variants were provided by the referring provider and classified using the American College of Medical Genetics and Genomics/Association for Molecular Pathology (ACMG/AMP) criteria for variant curation [12].

Cell culture

Primary skin fibroblasts from I-1, I-2, I-4, I-7, and I-9 were used. Fibroblasts were cultured in DMEM (Invitrogen) supplemented with 10% fetal bovine serum (Bodinco) and 1% penicillin–streptomycin (Invitrogen). Cultures were grown in 175-cm² culture flasks and maintained at 37°C in a humidified atmosphere of 5% CO₂. The medium was changed twice a week and the cultures were split at a 1:2 ratio whenever cells reached about 90% confluence. The cells were harvested with trypsin (Invitrogen) after reaching confluence, washed twice with Hank's buffered salt solution (Invitrogen). Two cell pellets were made from each flask and stored at –80°C.

Aminoacylation studies

Aminoacylation studies were performed as previously reported in Lenz et al. with modifications for the proteins being studied [13]. Cytosolic AlaRS and ArgRS activities were measured simultaneously in available patient fibroblast lysates, which were incubated at 37°C for 10 minutes in reaction buffer (50 mM Tris buffer [pH 7.5], 12 mM MgCl₂, 25 mM KCl, 1 mg/mL bovine serum albumin, 0.5 mM spermine, 1 mM ATP, 0.2 mM *E. coli* total tRNA, 1 mM dithiothreitol, 0.3 mM [D₃] alanine and 0.3 mM [¹⁵N₂] arginine). Aminoacyl-tRNA was precipitated with trichloroacetic acid (TCA). After washing free amino acids with TCA, [D₃] alanine and [¹⁵N₂] arginine were detached from the tRNA by addition of ammonia. [D₇] alanine and

[¹³C₆] arginine were added as internal standards. Labeled amino acids were quantified by liquid chromatography–tandem mass spectrometry (LC-MS/MS).

RESULTS

Clinical summaries of divergent presentations

Eleven individuals from ten families were seen at eight independent institutions and were evaluated for the possibility of an encephalopathy. In each of these cases, biallelic variants in *AARS1* were identified (Table 1).

Across this series, age at disease onset ranged from birth to 28 years of life. Six previously unreported individuals presented within the first four months of life, while the remaining four presented after the first year (12 months–27 years). All individuals developed a spastic tetraparesis over time. In most affected individuals, there was developmental delay (9/11), seizures (9/11), truncal hypotonia (8/11), and microcephaly (primary or secondary, 7/11). Four individuals had optic atrophy and vision loss over the course of their disease (Supplementary Fig. S1).

All seven individuals with early infantile-onset disease had epileptic encephalopathy, developmental delay, microcephaly, and hypotonia. Microcephaly was primary in five of seven cases and secondary in the remaining. These individuals did not achieve early developmental milestones (7/7) and were profoundly neurologically disabled. One individual (I-7) had congenital vertical talus, similar to the index cases [5]. There was no remarkable family history in any affected individual.

In this group of individuals with early infantile-onset disease, reported symptoms were primarily neurological although extra-neurological features were also seen. Feeding problems were prominent (6/7) with failure to thrive noted in six individuals and gastrostomy tube (g-tube) dependence in most cases (5/7). Gastroesophageal reflux (6/7) was also a common gastrointestinal complication of their neurologic disease. I-9 had hepatomegaly with elevated GGT on laboratory studies and periods of supraventricular paroxysmal tachycardia. Several patients had musculoskeletal complications from their neurologic disease. I-6a had congenital joint contractures and a congenital pulmonary airway malformation. I-8 was reported to have severe osteoporosis with at least one pathological fracture. Two individuals (I-6a and I-8) died from complications of their neurological disease at 8 months and 15 years of age; in I-8, this was noted to be due to complications from central respiratory failure. There were no other cardiac, respiratory, or gastrointestinal disturbances reported in these individuals.

In the individuals with late-onset disease, there was a significant range in age of disease onset. The eldest patient, I-1, presented at 27 years of age with severe headaches, dizziness, loss of balance, and blurred vision. She had a history of headaches early in adolescence. She had peripheral neuropathy and examination also revealed a wide-based gait with progressive left lower extremity spasticity and hyperreflexia. Last evaluated at 30 years of age, she had progressive cognitive decline, gait imbalance, peripheral vision loss, facial weakness, and dysarthria.

I-2 is a female with intrauterine growth retardation but normal growth and development in the first year of life. Best acquired motor development was supported walking. In the second year of life, she had a regression in speech and motor skills and had progressive spasticity of the upper and lower extremities. As the disease progressed, she developed severe spastic tetraparesis by 38 months of age that required an intrathecal baclofen pump placed over time. She developed neurogenic bladder and optic atrophy with loss of vision at 42 months and focal epilepsy at 4 years of age. She also suffered from chronic constipation, hip dislocation, scoliosis, pes equinovarus, and severe osteoporosis with pathologic fracture. Respiratory chain analysis in muscle tissue showed diminished activities for complexes I, II/III, and IV.

Table 1. AARS1 identified variants.

	Study ID	Zygosity	Variant (GRCh37)	cDNA change (NM_001605.2)	Protein change/ domain affected	gnomAD AF ^b	CADD ^c /SIFT/ Mutation Taster	ACMG/AMP variant classification	ACMG/AMP criteria ^d	Enzyme activity
Late-onset cases	I-1 ^a	Mat	16-70310906-T-C	c.296A>G	p.(Glu99Gly) Aminoacylation	0.0	32/D/DC	P	PS3, PM2, PM3, PP3	16% activity 0.218 nmol/ (min*mg protein)
		De novo	16-70304137-T-C	c.778A>G	p.(Thr260Ala) Aminoacylation	0.000004	27/D/DC	P	PS3, PS2, PM2, PM3, PP3	
	I-2	Pat	16-70305792-CT-TG	c.562_563delinsCA	p.(Ser188His) Aminoacylation	0.0	27/D/DC	P	PS3, PM2, PP3, PP4	35% activity 0.293 nmol/ (min*mg protein)
		Mat	16-70296346-C-T	c.1574G>A	p.(Cys525Tyr) Editing	0.0	25/T/DC	LP	PM2, PM3 PP3, PP4	
	I-3	Hom	16-70294991-C-T	c.1741G>A	p.(Gly581Ser) Editing	0.000007	25/D/DC	P	PM2, PM3, PP3, PP4	NA
Early infantile-onset cases	I-4 ^e	Pat	16-70292116-A-G	c.1997T>C	p.(Val666Ala) Editing	0.000005	25/D/DC	P	PS3, PM2, PM3, PP3, PP4	11% activity 0.137 nmol/ (min*mg protein)
		Mat	Exon 1-4 Deletion		p.? Aminoacylation	NA		P	PVS1, PM2, PM3	NA
	I-5	Pat	16-70289666-T-C	c.2251A>G	p.(Arg751Gly) Editing	0.000048	27/D/DC	P	PS1, PS3, PM2, PP3	NA
		Mat	16-70293063-G-C	c.1812C>G	p.(Asn604Lys) Editing	0.0	25/D/DC	LP	PM2, PM3, PP3, PP4	
	I-6a & I-6b	Hom	16-70289631-C-T	c.2286G>A	p.(Lys762 = / Ala763Valfs*11) ^e C-terminal	0.000004	23/NA /NA	P	PVS1, PS3, PM2, PM3, PP3, PP4	NA
	I-7	UNK	16-70302257-G-A	c.988C>T	p.(Arg330*) tRNA Recognition	0.0	37/NA/DC	P	PVS1, PM2, PP3	9% activity 0.067 nmol/ (min*mg protein)
		UNK	16-70286793-C-T	c.2738G>A	p.(Gly913Asp) C-terminal	0.00002	31/D/DC	LP	PS3, PM2, PP3, PP4	
	I-8	Pat	16-70310455-AAAGT-	c.410_413del	p.(Tyr137Leufs*9) Aminoacylation	0.0	32/NA/NA	LP	PVS1, PM2	NA
		Mat	16-70296331-T-C	c.1589A>G	p.(Asp530Gly) Editing	0.0	32/D/DC	LP	PM2, PM3, PP3, PP4	
	I-9	Pat	16-70310405-TC-	c.462_463del	p.(Gln154Hisfs*9) Aminoacylation	0.0	25/NA/NA	P	PVS1, PS3, PM2, PM3	15% activity 0.184 nmol/ (min*mg protein)
		Mat	16-70294991-C-T	c.1741G>A	p.(Gly581Ser) Editing	0.000004	25/D/DC	P	PS3, PM2, PM3, PP3, PP4	
	I-10	Mat	16-70302248-G-A	c.997C>T	p.(Arg333*) tRNA Recognition	0.000004	38/NA/DC	P	PVS1, PM2, PM3, PP4	NA
		Pat	16-70286793-C-T	c.2738G>A	p.(Gly913Asp) C-terminal	0.00002	31/D/DC	P	PS4, PS3, PM3, PP3, PP4, PP5	

ACMG/AMP American College of Medical Genetics and Genomics/Association for Molecular Pathology. AF allele frequency, cDNA complementary DNA, D damaging, DC disease-causing, Hom homozygous, LP likely pathogenic, Mat maternal, NA not available, P pathogenic, Pat paternal, T tolerated, UNK unknown.

^aSupport for the pathogenicity of the variants found in this individual is provided in the Supplemental Text.

^bAllele frequency determined from gnomAD v2.1.1.

^cMax CADD score at variant site if multiallelic variant.

^dACMG/AMP scoring criteria are described in Richards et al. [12].

^eVariant shown to affect splicing through RNA studies from peripheral blood with both a wild-type and an aberrantly spliced product detected. The aberrantly spliced products resulting r.2286G>A or r.2286delinsagagagcag maintain normal AARS1 splicing or result in the use of a new donor splice site from Exon 16 at c.2286 + 9_2286 + 10 and result in a frameshift in the transcribed protein.

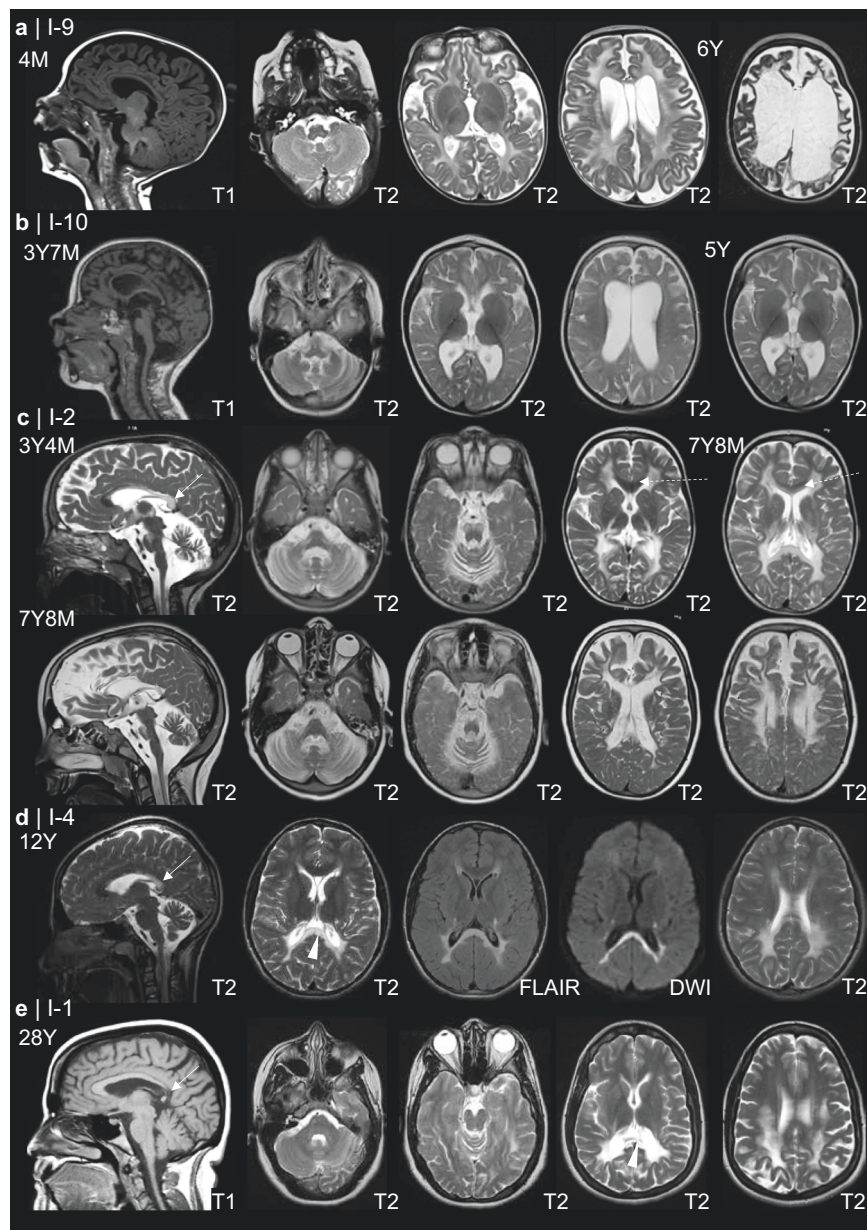


Fig. 1 Magnetic resonance image (MRI) findings in individuals with recessive *AARS1*-related disease. Evaluation of the neuroimaging findings between individuals with early infantile-onset disease in comparison to late-onset individuals. Sagittal and axial T₁ and T₂ weighted images were compared for all individuals. Diffusion-weighted and fluid-attenuated inversion recovery (FLAIR) images were compared where available. **(a, b)** In individuals with early infantile-onset there is early evidence of deficient myelination. At 4 months of age in I-9, there is absent myelination in early myelination structures, including the posterior limb of the internal capsule and mild ventriculomegaly suggesting a degree of cerebral volume loss. At 6 years, profound cerebral atrophy is seen. **(b)** Some individuals with early infantile-onset disease achieve a mild degree of myelination, but there is some cerebral atrophy and a persistent deficiency in myelination over time. **(c–e)** In individuals with late-onset disease, age at disease onset and neuroimaging features are more variable. In all individuals shown, there appears to be preferable involvement of the splenium of the corpus callosum seen on both sagittal (white arrow) and axial imaging (white arrowhead, **d** and **e**). **(c)** In the individual with late-onset disease and available follow-up imaging over time, there is progressive involvement to affect the frontal white matter and the remainder of the corpus callosum (dashed white arrow). There is also progressive cerebral atrophy. **(d)** There is progressive cerebral white matter involvement and areas of restricted diffusion in the affected periventricular white matter in cases with diffusion-weighted imaging obtained during the period of clinical decline. These features in late-onset disease were reminiscent of neuroimaging features seen *AARS2*-related disorder.

Electrophysiological studies showed pathologic evoked visual and somatosensory potentials. Laboratory studies showed chronic hypoalbuminemia. She was last evaluated at 12 years of age and had severe neurological impairment but a stable disease course.

I-3 presented at 36 months with regression in mobility, motor skills, and speech after a normal pregnancy, neonatal period, and early psychomotor development. She developed a severe spastic

tetraparesis with dystonia and had hip dislocations. She developed intractable focal epilepsy. On examination at 19 years of age she had microcephaly and remained alert and interactive. She had recurrent lower respiratory tract infections thought to be related to aspiration in her late teenage years and was transitioned to g-tube feedings. She died at 19 years of age as a result of central respiratory failure during a respiratory tract infection.

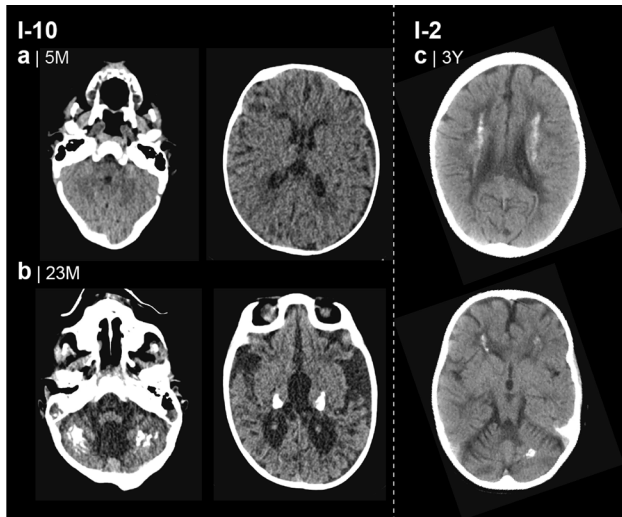


Fig. 2 Calcium deposits in *AARS1*-related disorder. (a) Computed tomography (CT) imaging of I-9 was performed at 5 months and 23 months of age. On early imaging studies calcifications were not evident, but (b) follow-up imaging at 23 months demonstrated calcifications in the cerebellum and thalami bilaterally. (c) CT in I-2 at 3 years of age reveals the presence of calcifications in the cerebral and cerebellar white matter.

I-4 developed normally in the first year of life, but mild development delays were noted in the second year of life after a suspected encephalopathic episode with no determined cause. During his initial encephalopathic episode he was noted to be hypoalbuminemic, which has since resolved. He started to walk autonomously at the age of 16 months and language delay resolved with speech therapy. He developed normally and remained healthy until 12 years of age when he had an abrupt onset of neurological symptoms with right-sided hemiparesis, which evolved to a tetraparesis over a two-week period, and was followed by significant motor and cognitive regression over the next five months. He also developed bradykinesia and dystonic movements. Communication was limited as he developed a severe spastic dysarthria but was able to understand simple commands.

Neuroimaging

Seventeen neuroimaging studies were available for review from eight affected individuals while in one case, only the clinical report of magnetic resonance image (MRI) findings was available. In three individuals, all with early infantile-onset disease, brain MRI showed deficient myelination in the earliest scans, where early myelinating structures such as the brainstem and posterior limb of the internal capsule (PLIC) suggest absent myelination from at the earliest study 4 months of age. In I-6a there was immature gyration, absent myelination, and evidence of early atrophy. I-9 had a brain MRI and computed tomography (CT) performed at 4 and 5 months of age, respectively (Figs. 1a and 2b). The earliest scans show absent myelination in early myelinating structures, including the cerebellum, brainstem, and PLIC, with early ventriculomegaly and enlarged subarachnoid spaces. A follow-up CT scan at 23 months of age revealed calcifications in the cerebellar white matter and the dentate nuclei (Fig. 2b). An MRI performed at 6 years and 5 months of age showed total cerebral white matter volume loss with profound ventriculomegaly and enlarged subarachnoid spaces.

The four individuals with late-onset disease all had a distinctly different white matter disease, characterized by a posterior predominant leukoencephalopathy (Fig. 1c–e). In all cases, the

splenium and the posterior aspect of the body of the corpus callosum (4/4) were significantly affected while the genu is spared in I-1 and I-4. In I-3, there was isolated involvement of the inner blade of the genu that progressed to total involvement on follow-up scans. The frontal white matter was spared in I-1 and I-4 (2/4) and the subcortical U-fibers were spared in all 4 individuals (4/4). There was extension of the white matter signal hyperintensity through the corticospinal tracts into the brainstem. In I-2 there was total involvement of the ventral midbrain structures, and progressive atrophy of these structures on follow-up imaging. There were areas of restricted diffusion in the affected periventricular white matter (2/3) and suspected tissue necrosis with white matter rarefaction seen on fluid-attenuated inversion recovery (FLAIR) (2/4). At three years of age in I-3 there was no evidence of rarefaction but on repeat imaging at six years there was extensive rarefaction of the cerebral white matter. Follow-up imaging in I-2 and I-3 suggested a progressive degenerative disease with marked atrophy affecting the cerebrum and cerebellum on repeat imaging scans. CT scan in I-2 revealed the presence of cerebral and cerebellar calcifications (Fig. 2c). No follow-up scans were available for I-1 and I-4 from their initial presentation, which showed evidence of active demyelination posteriorly and mild white matter volume loss. Magnetic resonance spectroscopy (MRS) in I-2 revealed elevated lactate and in I-4 showed peaks of choline and lactate and mild NAA reduction.

AARS1 variants identified

Across these 11 individuals from 10 unrelated families, 15 unique variants in *AARS1* were identified through next-generation sequencing (Table 1; *AARS1*, NM_001605.2), of which most were not previously reported in affected individuals. One individual (I-5) was compound heterozygous for a variant observed in the initial description of this condition, p.(Arg751Gly), found in *trans* with a unique missense variant (p.[Asn604Lys]). I-7 and I-10 each were compound heterozygous for p.(Gly913Asp) and a truncating variant (p.[Arg330*] and p.[Arg333*], respectively). The p.(Gly913Asp) variant was previously seen in the early infantile-onset form of *AARS1*-related disease [8, 9]. All other variants had not been previously identified in the literature or the ClinVar variant database. Two individuals, one with late and the other with early onset disease (I-3 and I-9, respectively), shared the same variant, p.(Gly581Ser). However, in I-3 the variant was found in the homozygous state, while in I-9 it was compound heterozygous with a frameshift variant (p.[Gln154Hisfs*9]). In I-6a/b, a homozygous synonymous variant shown to affect splicing through RNA studies from peripheral blood, producing both a wild-type and an aberrantly spliced product. The aberrantly spliced product created from r.2286delginsagugagcag results in the use of a new donor splice site from exon 16 at c.2286 + 9_2286 + 10 and results in a frameshift in the transcribed protein. All identified variants were absent or found at very low allele frequencies in the gnomAD population allele frequency database (range 0.0–0.00002), are predicted damaging across a suite of in silico tools and affect highly evolutionarily conserved residues (Table 1).

Missense variants identified in I-1 were associated with increased transcription and messenger RNA (mRNA) levels on reverse-transcription quantitative polymerase chain reaction (RT-qPCR, [Supplementary Fig. S2]). Despite increased mRNA levels, western blot showed reduced AlaRS protein levels (Supplementary Fig. S3), suggesting protein instability. In I-4, the p.(Val666Ala) variant and multiexonic deletion were found to cause decreased mRNA and protein level (Supplementary Fig. S4–S5). Moreover, the p.(Val666Ala) expressed in a yeast model deleted at the *AARS1* yeast orthologue, *ALA1* demonstrated reduced ability to rescue yeast growth relative to wild-type protein (Supplementary Fig. S6), supporting pathogenicity of this missense variant.

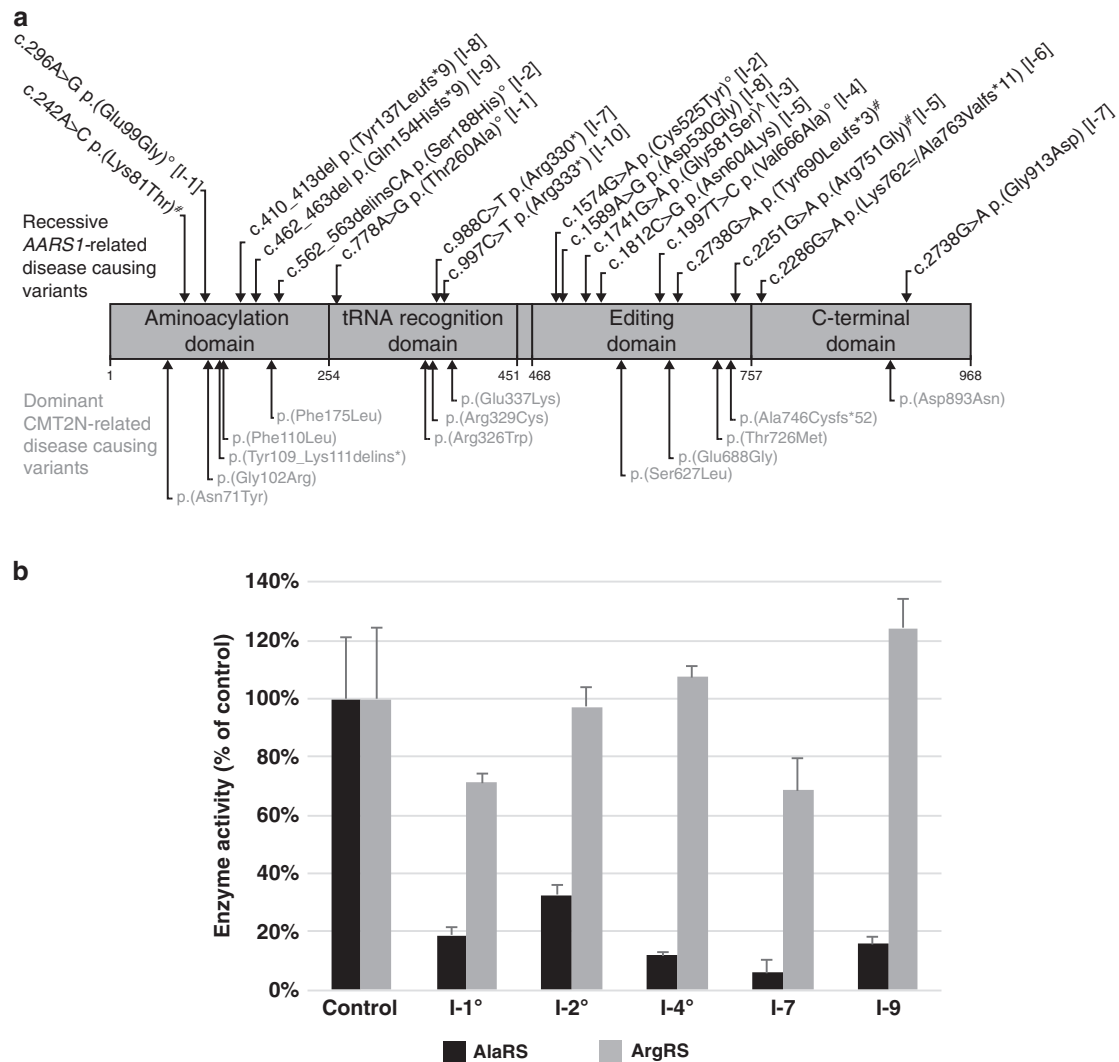


Fig. 3 Variants identified in this cohort and aminoacylation studies of affected individuals. **(a)** Schematic overview of the AlaRS functional domains and variants identified within this cohort. The amino acid changes caused by previously identified variants (Lys81Thr, Tyr690Leufs*3, and Arg751Gly) are marked with a #. One individual (I-4) was found to have a structural variant (not shown). Variants associated with late-onset disease are designated with a [°], variants designated with a [^] are seen in both phenotypes, and all other variants are associated with early infantile-onset disease. Variants below the domain markings and colored in gray are previously associated with autosomal dominant Charcot–Marie–Tooth disease, type 2N. **(b)** Aminoacylation studies performed in triplicate on fibroblast lysates from three individuals with late-onset AARS1-related disease noted with a [°] and two with the more severe early infantile-onset form shown diminished AlaRS activity relative to a control sample and using ArgRS activity as an in-sample control. Activity is more severely reduced in three individuals, including two (I-7 and I-9) with early infantile-onset disease and one individual (I-4) with later disease onset but a rapidly progressive course. Bars represent average \pm standard deviation.

Human AARS1 consists of four functional domains derived from sequence alignment and structural modeling: the aminoacyl-tRNA synthetase domain (residues 1–254), the tRNA recognition domain (residues 255–451), the editing domain (residues 468–757), and the oligomerization (C-terminal) domain (residues 758–968), also known as C-Ala. No discernible genotype–phenotype relationship could be identified based on variant location since the identified variants fell across all domains of the protein (Figure 3a). It is remarkable that all but one (I-5) early onset patients had at least one variant resulting in a structurally alternative protein (nonsense or frameshift variants).

Defective aminoacylation

AlaRS activity was measured in cytoplasmic fractions isolated from fibroblasts of three of the four affected individuals with late-onset

disease and performed on two individuals with early infantile-onset AARS1-related disease. Fibroblasts were not available from the remaining individuals. In all individuals studied, AlaRS activity was reduced. In the late-onset group, AlaRS residual activity was found to be 16%, 35%, and 11% of controls in I-1, I-2, and I-4 respectively (Figure 3b). In I-7 and I-9 from the early infantile-onset group, AlaRS activity was measured to be 9% and 15% in those individuals, respectively. Arginyl-tRNA synthetase (ArgRS encoded by *RARS1* [OMIM 107820]) activity, measured as an internal control, was within control values for all affected individuals tested.

DISCUSSION

While many disorders associated with *-ARS1* variants were first described with isolated phenotypes, wider clinical variation is

increasingly recognized. In this series, we present clinical and molecular data on an additional 11 cases of *AARS1*-related disease. Analysis of these individuals identified two groups on the basis of age at disease onset and presentation of neuroimaging findings. Early infantile-onset recessive *AARS1*-related cases presented similarly to the patients previously described in Simons et al. [5], and Nakayama et al. [8]. A separate group of individuals with onset of disease beyond the first year of life and a distinctly different neuroradiologic phenotype emerged, indicating also wider neuroradiologic variation. Our findings broaden the clinical and the genetic spectrum associated with recessive *AARS1* variants beyond early infantile-onset epileptic encephalopathy with deficient myelination.

In our series, several individuals had compound heterozygous variants where one allele was distinctly classified as likely pathogenic or pathogenic based on the ACMG/AMP criteria. To the best of our knowledge, heterozygotes of these alleles did not display any neurological signs of CMT2N and thus it is possible that in these individuals, the reduced aminoacylation activity associated with the variant allele is compensated for by the activity associated with the wild-type allele. In addition, to-date no reported pathogenic or likely pathogenic *AARS1* variant causing CMT2N as listed on ClinVar has also been associated as a disease-causing variant in recessive disease (Fig. 3a). Thus, there does not appear to be a genotype–phenotype correlation predicting whether an *AARS1* variant would be causative of either dominant or recessive *AARS1*-related disease, nor does there appear to be a correlation between the residual enzyme activity and the severity of the disease or the age of onset. Even though cases in the early presenting group more commonly involved frameshift/truncating variants, AlaRS activities were similar, rendering differences in canonical function an implausible explanation. More recently, there has been a report of a single family where a heterozygous variant in *AARS1* was suspected to be the cause of a late-onset hereditary diffuse leukoencephalopathy with spheroids of the Swedish type (HDLS-S) in an extensive family [14]. As there is further expansion of both dominant and recessive forms of *AARS1*-related disease, the possibility and threshold of compensation remains an intriguing clinical question.

While our assessment is limited to the combined 15 individuals in the present study and those previously reported [5, 8–11], a diverging clinical presentation is evident and should be considered in the diagnostic workup of similar patients. Further it should be noted that late-onset *KARS1*-, *AARS1*-, and *AARS2*-related disease share similar MRI features and may confound gene-specific diagnostic approaches. Finally, it bears mentioning that the overlap between late-onset *AARS1*- and *AARS2*-related disease is strikingly similar to age-specific MRI patterns seen in disorders affecting the aspartyl-tRNA synthetase, encoded by *DARS1* (OMIM 603084) and *DARS2* (OMIM 610956) [6]. In our late-onset *AARS1*-related cases, neuroimaging demonstrated involvement of the corpus callosum with lacunar like injury, cerebral white matter involvement with progressive atrophy and areas of restricted diffusion in the affected periventricular white matter in cases with diffusion-weighted imaging obtained during clinical decline (Fig. 1c, d) [15]. These findings are very reminiscent of MRI patterns seen in *AARS2*-related leukoencephalopathy, suggesting the possibility of differences in MRI based on age of presentation in disorders affecting the AlaRS.

-ARS1 variants almost invariably have a predilection for involvement of the CNS white matter. Almost all of the cytoplasmic aARS enzymes that have been implicated in genetic disease have been associated with a prominent white matter phenotype [3, 4, 6, 16, 17]. In the index cases of recessive *AARS1*-related disease, there was an apparent deficiency and arrest in myelination from disease onset, with only mild progression of

myelination in early myelinating structures in one individual [5]. This phenotype is recapitulated in most affected individuals in our study ($n=6$). In individuals with late-onset disease, MRI demonstrated a prominent leukoencephalopathy, with posterior involvement affecting the splenium of the corpus callosum, PLIC, and extending through the corticospinal tracts. This appears to be progressive over time, invariably affecting the genu of the corpus callosum and extending to the frontal white matter in two individuals. Further studies including longitudinal imaging and clinical follow-up will be valuable in understanding the progression of features in this disorder.

DATA AVAILABILITY

De-identified data are available upon request by contacting the Leukodystrophy Center at Children's Hospital of Philadelphia at <https://www.chop.edu/centers-programs/leukodystrophy-center/contact>.

Received: 4 April 2021; Revised: 8 July 2021; Accepted: 9 July 2021;

Published online: 27 August 2021

REFERENCES

- Meyer-Schuman R, Antonellis A. Emerging mechanisms of aminoacyl-tRNA synthetase mutations in recessive and dominant human disease. *Hum Mol Genet*. 2017;26:R114–27.
- Antonellis A, Green ED. The role of aminoacyl-tRNA synthetases in genetic diseases. *Ann Rev Genomics Hum Genet*. 2008;9:87–107.
- Fuchs SA, Schene IF, Kok G, Jansen JM, Nikkels P, van Gassen K, et al. Aminoacyl-tRNA synthetase deficiencies in search of common themes. *Genet Med*. 2019;21:319–30.
- Wolf NI, Salomons GS, Rodenburg RJ, Pouwels PJ, Schieving JH, Derks TG, et al. Mutations in RARS cause hypomyelination. *Ann Neurol*. 2014;76:134–9.
- Simons C, Griffin LB, Helman G, Golas G, Pizzino A, Bloom M, et al. Loss-of-function alanyl-tRNA synthetase mutations cause an autosomal-recessive early-onset epileptic encephalopathy with persistent myelination defect. *Am J Hum Genet*. 2015;96:675–81.
- Taft RJ, Vanderver A, Leventer RJ, Damiani SA, Simons C, Grimmond SM, et al. Mutations in DARS cause hypomyelination with brain stem and spinal cord involvement and leg spasticity. *Am J Hum Genet*. 2013;92:774–80.
- Shashi V, Schoch K, Spillmann R, Cope H, Tan QK, Walley N, et al. A comprehensive iterative approach is highly effective in diagnosing individuals who are exome negative. *Genet Med*. 2019;21:161–72.
- Nakayama T, Wu J, Galvin-Parton P, Weiss J, Andriola MR, Hill RS, et al. Deficient activity of alanyl-tRNA synthetase underlies an autosomal recessive syndrome of progressive microcephaly, hypomyelination, and epileptic encephalopathy. *Hum Mutat*. 2017;38:1348–54.
- Krey I, Krois-Neudenberg J, Hentschel J, Syrbe S, Polster T, Hanker B, et al. Genotype-phenotype correlation on 45 individuals with West syndrome. *Eur J Paediatr Neurol*. 2020;25:134–8.
- Karakaya M, Störbeck M, Strathmann EA, Delle Vedove A, Höcker I, Altmueller J, et al. Targeted sequencing with expanded gene profile enables high diagnostic yield in non-5q-spinal muscular atrophies. *Hum Mutat*. 2018;39:1284–98.
- Marten LM, Brinkert F, Smith DEC, Prokisch H, Hempel M, Santer R. Recurrent acute liver failure in alanyl-tRNA synthetase-1 (AARS1) deficiency. *Mol Genet Metab Rep*. 2020;25:100681.
- Richards S, Aziz N, Bale S, Bick D, Das S, Gastier-Foster J, et al. Standards and guidelines for the interpretation of sequence variants: a joint consensus recommendation of the American College of Medical Genetics and Genomics and the Association for Molecular Pathology. *Genet Med*. 2015;17:405–24.
- Lenz D, Smith DEC, Crushell E, Husain RA, Salomons GS, Alhaddad B, et al. Genotypic diversity and phenotypic spectrum of infantile liver failure syndrome type 1 due to variants in LARS1. *Genet Med*. 2020;22:1863–73.
- Sundal C, Carmona S, Yhr M, Almström O, Ljungberg M, Hardy J, et al. An AARS variant as the likely cause of Swedish type hereditary diffuse leukoencephalopathy with spheroids. *Acta Neuropathol Commun*. 2019;7:188.
- Dallabona C, Diodato D, Kevelam SH, Haack TB, Wong LJ, Salomons GS, et al. Novel (ovario) leukodystrophy related to AARS2 mutations. *Neurology*. 2014;82:2063–71.
- Zhou XL, He LX, Yu LJ, Wang Y, Wang XJ, Wang ED, et al. Mutations in KARS cause early-onset hearing loss and leukoencephalopathy: potential pathogenic mechanism. *Hum Mutat*. 2017;38:1740–50.

17. Mendes MI, Green LMC, Bertini E, Tonduti D, Aiello C, Smith D, et al. RARS1-related hypomyelinating leukodystrophy: expanding the spectrum. *Ann Clin Transl Neurol.* 2020;7:83–93.

ACKNOWLEDGEMENTS

We thank the patients and their families. G.H. was supported by the Ochsner MD-PhD scholarship and a MCRI PhD Top-Up Scholarship. The participation of G.H. and C.S. is in part financed by the Australian National Health and Medical Research Council (NHMRC 1068278). The research conducted at the Murdoch Children's Research Institute was supported by the Victorian Government's Operational Infrastructure Support Program. This work was supported by the Italian Ministry of Health, grant RF-2016-02361241 (to E.B. and P.G.). T.B.H. was supported by the Deutsche Forschungsgemeinschaft (DFG, German Research Foundation)–Projektnummer (418081722). This study was partly supported by a grant from the Canadian Institutes of Health Research to G.B. (CIHR; 201610PJT-377869). G.B. has received the CIHR New Investigator Salary Award (2017–2022).

AUTHOR CONTRIBUTIONS

G.H., A.V., R.A.H. were responsible for conceptualization and supervision of the project. G.H. wrote the first draft and performed data curation, investigation, determined the methodology and performed formal analysis. M.I.M., F.N., L.D., O.S., T.M., A.D., A.P., R.C., A.T., M.C., C.A., P.G., S.F., D.E.C.S., K.H., A.H., S.B., I.B., U.K., D.G., T.A.G., F.E., K.S., R.G., E.B., I.T., R.J.T., R.S., U.B., T.B.H., G.S.S., C.S., G.B., and M.S.v.d.K. performed formal analysis and investigation. A.P., I.B., D.G., T.A.G., F.E., K.S., I.T., R.J.T., T.B.H., and C.S. performed variant curation. R.C., E.B., R.J.T., G.B., M.S.v.d.K., and A.V. performed funding acquisition. All authors reviewed and approved the manuscript prior to submission.

ETHICS DECLARATION

Patients and their families were collected prospectively in the Myelin Disorders Bioregistry. Project (MDBP) with approval from the institutional review board at Children's Hospital of Philadelphia (IRB Approval #IRB 14-011236). Written informed consent for collection of clinical information, neuroimaging, and genetic information was obtained for each study participant.

COMPETING INTERESTS

The authors declare no competing interests.

ADDITIONAL INFORMATION

Supplementary information The online version contains supplementary material available at <https://doi.org/10.1038/s41436-021-01286-8>.

Correspondence and requests for materials should be addressed to A.V. or R.A.H.

Reprints and permission information is available at <http://www.nature.com/reprints>

Publisher's note Springer Nature remains neutral with regard to jurisdictional claims in published maps and institutional affiliations.

Supplemental Text: A supplemental text with results regarding validation of variants identified in I-1 and I-4 is provided.